Using geometry to enhance the nonlinear response of quantum confined systems

Shoresh Shafei, Rick Lytel and Mark G. Kuzyk

Department of Physics and Astronomy, Washington State University, Pullman, Washington 99164-2814

ABSTRACT

We study the effect of geometry on the nonlinear response of a network of quantum wires that form loops. Exploiting the fact that a loop's transition moment matrix and energies are exactly solvable for each wire segment, they can be pieced together to determine the loop's properties. A Monte Carlo method is used to sample the configuration space of all possible geometries to determine the shape that optimizes the intrinsic hyperpolarizability. We suggest that a combination of wire geometry and confinement effects can lead to artificial systems with ultra-large nonlinear response, which can be potentially made using known nanofabrication techniques.

Keywords: hyperpolarizability, fundamental limit, quantum confined systems, quantum wire, nonlinear optical quantum graphs, sum rules

1. INTRODUCTION

Nonlinear optical materials have extensive applications in many areas of science and technology including all-optical switching,[1] 3-D photolithography,[2] quantum information,[3] optical data storage[4] and photodynamic cancer therapies,[5] to name a few. The study of these materials also provides insights with regards to the basic science of the systems with large nonlinear optical response.[6–9]

While many studies have attempted to identify the nonlinear optical properties of specific materials (see for example[10–12]), the theory of fundamental limits (FL) of the first and second hyperpolarizabilities has focused on understanding the general characteristics of quantum models, for which the nonlinear optical response is optimized.[13] The theory's fundamental assumption is called three-level ansatz and states that, when the hyperpolarizability of a quantum system is at its limit, only three quantum states contribute to the nonlinear response.[14,15] While this assumption has not been proven mathematically, it is supported by a large number of experimental and numerical results. See Refs.[16,17] for detailed discussion.

Sum rules also play a significant role in the theory of FL. As a powerful tool, sum rules relate the transition moments between different energy eigenstates, x_{ij}, to the energy values, e_i, through the following relation,

$$\sum_{n=0}^{\infty}\left(E_n-\frac{E_m+E_p}{2}\right)x_{mn}x_{np}=\frac{\hbar^2}{2m}\delta_{mp} \tag{1}$$

where m and p are the energies of the eigenstates of the system, δ_{mp} is the Kronecker delta and m is electron's mass. It should be noted that all discrete and continuum states and/or degenerate and non-degenerate states should be taken into account in sum over states in Eq. 1.[18]

Sum rules have widely been applied in the theory of FL. They were used to calculate the fundamental limit of the first, β_{max}, and second hyperpolarizability, γ_{max}, given by

$$\beta_{max}=3^{1/4}\left(\frac{e^3\hbar^3}{m^{3/2}}\right)\frac{N^{3/2}}{E_{10}^{7/2}} \tag{2}$$

email: shafei@wsu.edu

Optical Processes in Organic Materials and Nanostructures, edited by Rachel Jakubiak, Manfred Eich, Jean-Michel Nunzi, Proc. of SPIE
Vol. 8474, 84740P · © 2012 SPIE · CCC code: 0277-786/12/$18 · doi: 10.1117/12.928874

and

$$\gamma_{max} = 4\left(\frac{e^4\hbar^4}{m^2}\right)\frac{N^2}{E_{10}^5} \tag{3}$$

respectively, to find a dipole-free sum over states expression for the nonlinear hyperpolarizabilities,[19] and as a constraint on energies and transition moments in Monte Carlo simulations of β[16] and γ.[17] In Eqs. 2 and 3, the variables are, N, the number of electrons, and E_{10}, the energy difference between the first excited state and the ground state.

Originating from the fact that sum rules are direct consequences of quantum mechanics,[20] they can be used to verify the solution of the Schrödinger equation, whenever the corresponding Hamiltonian verifies the following relation:

$$\langle m\,|[x,[H,x]]|\,p\rangle = \frac{\hbar^2}{2m}\delta_{m,p} \tag{4}$$

where $|m\rangle$ and $|p\rangle$ are the Hamiltonian eigenstates. In an early work, Hadjimichael *et al.* showed that the conventional picture of the rigid rotator, in which the rotator's radius is assumed constant, does not comply with sum rules.[21] The authors then impose the uncertainty principle, use a highly weighted delta function potential in the radial direction, and take into account the radial component of the wavefunction to verify sum rules.

In another work, a system of one-electron inside a one-dimensional quantum wire embedded in two-dimensional space is investigated.[22] A highly-weighted and attractive delta function potential of the form

$$V(\tau) = -g\delta(\tau) \tag{5}$$

is employed in transverse direction of the wire, denoted by τ. In this model, it is assumed that $g \to \infty$, to make sure that at the limit of full confinement, electron is tight to the wire. The authors use sum rules to verify the solution of the Schrödinger equation for the particle inside a box of width a and in the presence of delta function potential. then, sum rules are verified for the electron inside the quantum wire for both transverse and longitudinal components. The authors show that at the limit of full confinement, the transverse component of the wavefunction is vital to verify sum rules, however, it does not play a role in the nonlinear optical response of the quantum wires.[22]

As one of the significant consequences of the theory of fundamental limits, it is shown that in ideal quantum models with large hyperpolarizabilities, the energy states become farther apart with increasing the number of states.[23] For instance, for particle in the box model, which potentially can yield very large hyperpolarizabilities, energy states are proportional to $E_n \propto n^2$. On the other hand, for Hydrogen atom-like systems, where $E_n \propto n^{-2}$, the energy states become denser when n increases, leading to low values of the hyperpolarizabilities.

Figure 1 illustrates the distribution of intrinsic first hyperpolarizability, β_{int}, for the two energy spectra discussed above. β_{int}, defined as

$$\beta_{int} = \frac{\beta}{\beta_{max}}, \tag{6}$$

is a scale-invariant quantity, and can be used to compare the hyperpolarizability of atoms and molecules with different shapes and sizes.[24] For each energy spectrum in Fig. 1, different colors correspond to different total number of energy states involved in the simulations, i.e. $n = 3, 4, 5, 20$. The largest attainable β_{int} for $E_n \propto n^{-2}$ is about 0.3 while the one for $E_n \propto n^2$ approaches the unity. According to Eq. 6 this implies that β for the particle in a box-like systems can potentially approach the fundamental limit, β_{max}.

The different behavior of three-level model systems in Fig. 1 is also interesting. When more than 3 states are involved in the simulation, β_{int} peaks at zero and moving to the limit, the frequency of occurring 4+ states decreases substantially. On the other hand, the large population of β_{int} values when only three levels are involved approach the limit. Vertical dashed lines represent the maximum attainable β_{int} allowed by the theory of FL. For detailed analysis read the Ref.[23]

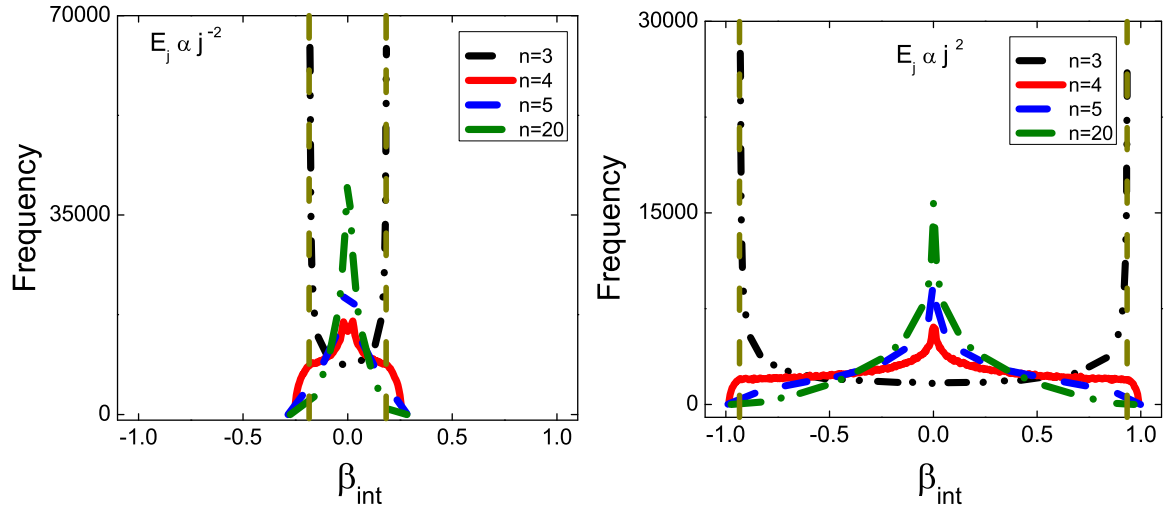

Figure 1. β_{int} distribution for two energy spectra. Frequency refers to the number of times that a specific value of β_{int} appears in the simulation. Source: Ref.[23]

The known materials do not have the requirements imposed by the theory of FL in order to yield large nonlinearities. Therefore people have turned their attention to artificial materials that can be synthesized in laboratories and their properties can be manipulated. Quantum dots, where the particles are confined in three dimensional space, e.g. inside a sphere, are the most well-known class of artificial materials.[25] To feel the confinement effects, the dimensions of the confining sphere should be comparable with the intrinsic length of the confined particles.

Mentioning some early works, it was Frohlich that discussed how the size of metallic particles affects their electronic conduction band.[26] Kubo showed that the confinement affects the properties of fine particles such as heat capacity, and paramagnetic susceptibility.[27] Rice *et al.* estimated the size threshold where small particles lose the bulk properties.[28] To review the topic read references.[29,30]

In nonlinear optics, people are interested in the relation between the confinement effects and the nonlinear optical response of these engineered materials. In a seminal work and based on the past experimental results of Schmidt-Ott *et al.*,[31] Jain and Lind[32] and Yao *et al.*,[33] Hache *et al.* assigned the second order nonlinearity of the metallic particles to the electrons confined inside the particles and calculated that this nonlinearity is proportional to a^{-3}, where a is the radius of the metallic particles.[34]

Artificial materials provide excellent opportunities to test the consequences of the theory of FL. Consider a single quantum wire. Such a system possesses the necessary requirement to achieve large nonlinear response: the energy spectrum for particles moving inside this wire is similar to the particle in a box model. In fact we are interested to use a network of such quantum wires, in order to form quantum graphs, and then show that not only the confinement effects but geometry also plays a significant role in determining the nonlinear optical response of the quantum graphs, providing a new opportunity to design materials with more efficient nonlinear properties.

In the next section, we explain the quantum mechanics of nonlinear optical quantum graphs, and then show that the effect of geometry can lead to nonlinearities that are larger than the nonlinear response of the best chromophores.

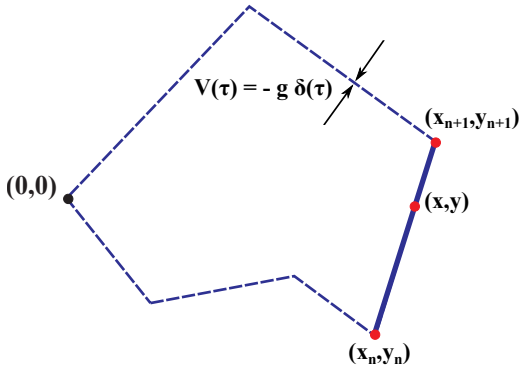

Figure 2. A typical quantum loop made out of 6 wire segments. Source: Ref.[35]

2. QUANTUM LOOPS AND THE EFFECT OF GEOMETRY

The quantum wires described in previous sections are used to form quantum graphs (Fig. 2). A highly weighted delta potential at transverse direction of each wire segment helps to vanish the confinement effects on the optical properties. The electron moves freely along the loop and at each node, i.e. when two wire segments connect, electron smoothly moves from one segment to the other one. In this work we only consider the quantum loops with periodic boundary conditions.

To ensure the viability of the results, we have developed a formalism for sum rules in 2-D, which is given by,

$$\sum_{n=-\infty}^{\infty}\sum_{\nu=-\infty}^{\infty}\left(E_{n\nu}-\frac{E_{p\kappa}+E_{q\lambda}}{2}\right)x_{p\kappa,n\nu}x_{n\nu,q\lambda}=\frac{\hbar^2}{2m}\delta_{pq}\delta_{\kappa\lambda}. \tag{7}$$

where Greek and Latin letters denote transverse and longitudinal components, respectively. $E_{p\kappa}=E_p+E_\kappa$, is sum of the energy of pth longitudinal and κth transversal states. The detailed analysis of the sum rules in 2-D has been discussed elsewhere.[35] We calculate the transition moments and energies of the quantum loops, and introduce them to the left-hand-side of Eq. 7. Table 1 presents the results for several randomly chosen triangles, as simple quantum graphs. Taking into account a larger number of longitudinal and transverse states in the numerical calculation reduces the uncertainty such that the final result for diagonal components, $p=q$ and $\kappa=\lambda$ in Eq. 7, is exactly equal to $\hbar^2/2m$, and zero otherwise.

The next step is to employ the transition moments and energies to calculate β_{int} values for different loops. Two remarks needs to be made. First, the transition moments turn out to be a function of the orientation of the graph, and consequently, the nonlinear optical response will depend on the geometry of the quantum loop. Second, β is not a scale-invariant quantity and therefore, we use β_{int} which was introduced in Eq. 6. It is given by,

$$\beta_{int} \equiv \frac{\beta}{\beta_{max}}=\left(\frac{3}{4}\right)^{3/4}{\sum_{n,m}}'\frac{\xi_{0n}\xi_{nm}\xi_{m0}}{e_n e_m}, \tag{8}$$

where ξ_{ij} and e_i are normalized transition moments and energies, defined by

$$\xi_{ij}=\frac{x_{ij}}{x_{01}^{max}}, \qquad e_i=\frac{E_{i0}}{E_{10}}, \tag{9}$$

and

$$x_{01}^{max}=\left(\frac{\hbar^2}{2mE_{10}}\right)^{1/2}. \tag{10}$$

Table 1. Verifying diagonal sum rules for different triangles as the simplest loops. The results in the sum rules column should be multiplied by $\hbar^2/m$. Source: Ref.[35]

Triangle Coordinates $(x_0, y_0, x_1, y_1, x_2, y_2)$	Sum Rules
(23,-16,3,-19,24,-15)	0.496
(18,-7,21,1,-25,-20)	0.495
(-32,-21,-49,-42,-69,-88)	0.496
(3,-93,-13,36,35,20)	0.496
(-7,-16,-27,64,42,-23)	0.495

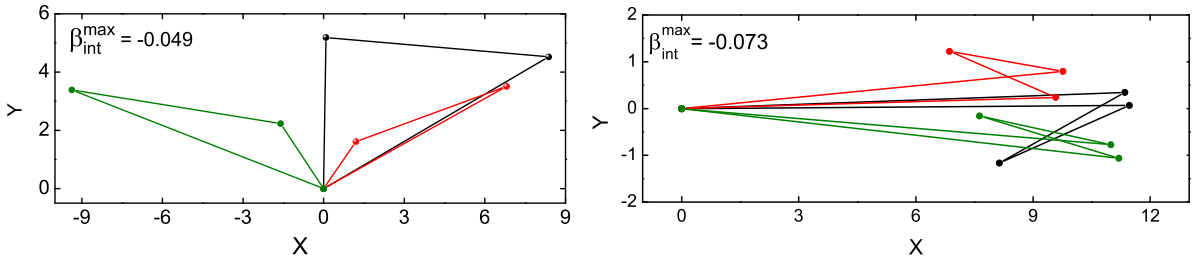

Figure 3. Three different triangles, left, and 4-segment loops, right, that lead to largest β_{int}. Source: Ref.[35]

x_{01}^{max} represents the largest possible transition moment.

We use the Monte Carlo simulations to generate a distribution of β_{int} values for thousands of triangles and 4-segment quantum loops. Figure 3 left illustrates the three triangles with the best intrinsic hyperpolarizabilities. The largest attainable $|\beta_{int}| \equiv 0.05$. However small, the geometry contribution to the nonlinear response, in the absence of the confinement effects, is larger than β_{int} for the best molecules known. On the other hand, β_{int} for 4-segment loops gets even better. The best values are about $|\beta_{int}| \equiv 0.073$ and belongs to the quantum loops represented in Fig. 3 right. It should be noted that the wire segments in 4-segment loop are assumed non-interacting. The promising technological advances in the field of semiconductor nanowires will enable us to design and fabricate of such quantum graphs in the near future,[36] providing a great opportunity for the field of nonlinear optical materials.

3. CONCLUSION

While the role of quantum confinement in enhancing the nonlinear response of quantum-confined systems has been widely studied in the literature, no detailed study has ever addressed the role of other parameters like the geometry or topology. In this paper we continued our effort to determine the effect of geometry on quantum graphs for triangles and extended it to 4-segment loops. For a one-electron model in a quantum loop, we showed that the intrinsic hyperpolarizability is a function of the orientation of every single wire segment with respect to the coordinate axis. We used this fact and employed the numerical methods to find the best graphs with largest hyperpolarizabilities. Future attempts will focus on more complicated graphs, as well as generalizing the model to include many electrons.

ACKNOWLEDGMENTS

S. Shafei and M. G. Kuzyk would like to thank the National Science Foundation (NSF) (ECCS-1128076) for generously supporting this work.

REFERENCES

[1] J. Hales, J. Matichak, S. Barlow, S. Ohira, K. Yesudas, J. Brédas, J. Perry, and S. Marder, "Design of polymethine dyes with large third-order optical nonlinearities and loss figures of merit," *Science* **327**(5972), p. 1485, 2010.

[2] S. Kawata, H.-B. Sun, T. Tanaka, and K. Takada, "Finer features for functional microdevices," *Nature* **412**, pp. 697–698, 2001.

[3] A. Feizpour, X. Xing, and A. Steinberg, "Amplifying single-photon nonlinearity using weak measurements," *Phys. Rev. Lett.* **107**(13), p. 133603, 2011.

[4] B. H. Cumpston, S. P. Ananthavel, S. Barlow, D. L. Dyer, J. E. Ehrlich, L. L. Erskine, A. A. Heikal, S. M. Kuebler, I.-Y. S. Lee, D. McCord-Maughon, J. Qin, H. Rockel, M. Rumi, X.-L. Wu, S. Marder, and J. W. Perry, "Two-photon polymerization initiators for three-dimensional optical data storage and microfabrication," *Nature* **398**, pp. 51–54, 1999.

[5] I. Roy, T. Y. Ohulchanskyy, H. E. Pudavar, E. J. Bergey, A. R. Oseroff, J. Morgan, T. J. Dougherty, and P. N. Prasad, "Ceramic-Based Nanoparticles Entrapping Water-Insoluble Photosensitizing Anticancer Drugs: A Novel Drug-Carrier System for Photodynamic Therapy," *J. Am. Chem. Soc.* **125**, pp. 7860–7865, 2003.

[6] S. R. Marder, D. N. Beratan, and L.-T. Cheng, "Approaches for optimizing the first electronic hyperpolarizability of conjugated organic molecules," *Science* **252**, pp. 103–06, 1991.

[7] F. Meyers, S. R. Marder, B. M. Pierce, and J. L. Bredas, "Electric Field Moldulated Nonlinear Optical Properties of Donor-Acceptor Polyenes: Sum-over-States Investigation of the Relationship between Molecular Polarizabilities (α, β, and γ) and Bond Length Alteration," *J. Amer. Chem. Soc.* **116**(23), pp. 10703–14, 1994.

[8] J. Zhou, M. G. Kuzyk, and D. S. Watkins, "Pushing the hyperpolarizability to the limit," *Opt. Lett.* **31**, p. 2891, 2006.

[9] J. Zhou, U. B. Szafruga, D. S. Watkins, and M. G. Kuzyk, "Optimizing potential energy functions for maximal intrinsic hyperpolarizability," *Phys. Rev. A* **76**, p. 053831, 2007.

[10] S. D. Bella, I. Fragala, I. Ledoux, M. A. D-Garicia, P. G. Lacroix, and T. J. Marks, "Sizable Second-Order Nonlinear Optical Response of Donor-Acceptor Bis(salicylaldiminator)nickel(II) Schiff Base Complexes," *Chem. Matter* **6**, pp. 881–883, 1994.

[11] D. B. Studebaker, G. T. Stauf, T. H. Baum, T. J. Marks, H. Zhou, and G. K. Wong, "Second Harmonic Generation from Beta Barium Borate (b-BaB2O4) Thin Films Grown by Metallorganic Chemical Vapor Deposition," *Appl. Phys. Lett.* **70**(5), pp. 565–7, 1997.

[12] H. Kang, A. Facchetti, P. Zhu, H. Jiang, Y. Yang, E. Cariati, S. Righetto, R. Ugo, C. Zuccaccia, A. Macchioni, C. L. Stern, Z. Liu, S. T. Ho, and T. J. Marks, "Exceptional Molecular Hyperpolarizabilities in Twisted π-Electron System Chromophores," *Angew. Chem. Int. Ed.* **44**, pp. 7922–7925, 2005.

[13] M. G. Kuzyk, "Using fundamental principles to understand and optimize nonlinear-optical materials," *J. Mat. Chem.* **19**, pp. 7444–7465, 2009.

[14] M. G. Kuzyk, "Physical Limits on Electronic Nonlinear Molecular Susceptibilities," *Phys. Rev. Lett.* **85**, p. 1218, 2000.

[15] M. G. Kuzyk, "Fundamental limits on third-order molecular susceptibilities," *Opt. Lett.* **25**, p. 1183, 2000.

[16] M. C. Kuzyk and M. G. Kuzyk, "Monte Carlo Studies of the Fundamental Limits of the Intrinsic Hyperpolarizability," *J. Opt. Soc. Am. B.* **25**(1), pp. 103–110, 2008.

[17] S. Shafei, M. C. Kuzyk, and M. G. Kuzyk, "Monte carlo studies of the intrinsic second hyperpolarizability," *J. Opt. Soc Am. B* **27**, pp. 1849–1856, 2010.

[18] F. Fernández, "The thomas-reiche-kuhn sum rule for the rigid rotator," *Int. J. Math. Ed. Sc. Tech.* **33**(4), pp. 636–640, 2002.

[19] M. G. Kuzyk, "Compact sum-over-states expression without dipolar terms for calculating nonlinear susceptibilities," *Phys. Rev. A* **72**, p. 053819, 2005.

[20] H. A. Bethe and E. E. Salpeter, *Quantum Mechanics of One and Two Electron Atoms*, Plenum, New York, 1977.
[21] E. Hadjimichael, W. Currie, and S. Fallieros, "The thomas–reiche–kuhn sum rule and the rigid rotator," *Am. J. Phys.* **65**(4), pp. 335–341, 1997.
[22] S. Shafei and M. G. Kuzyk, "The effect of extreme confinement on the nonlinear-optical response of quantum wires," *J. Nonl. Opt. Phys. Mat.* **20**, pp. 427–441, 2011.
[23] S. Shafei and M. G. Kuzyk, "Critical role of the energy spectrum in determining the nonlinear-optical response of a quantum system," *J. Opt. Soc. Am. B* **28**, pp. 882–891, 2011.
[24] M. G. Kuzyk, "A birds-eye view of nonlinear-optical processes: Unification through scale invariance," *Nonl. Opt. Quant. Opt.* **40**, pp. 1–13, 2010.
[25] R. Ashoori, "Electrons in artificial atoms," *Nature* **379**(6564), pp. 413–419, 1996.
[26] H. Frohlich, "Die spezifische wärme der elektronen kleiner metallteilchen bei tiefen temperaturen," *Physica* **4**(5), pp. 406–412, 1937.
[27] R. Kubo, "Electronic properties of metallic fine particles. i.," *J. Phys. Soc. Jap.* **17**(6), pp. 975–986, 1962.
[28] M. J. Rice, W. R. Schneider, and S. Strässler, "Electronic polarizabilities of very small metallic particles and thin films," *Phys. Rev. B* **8**, pp. 474–482, Jul 1973.
[29] M. Kastner, "Artificial atoms," *Physics Today* , p. 25, 1993.
[30] K. Likharev, "Single-electron devices and their applications," *Proc. IEEE* **87**(4), pp. 606–632, 1999.
[31] A. Schmidt-Ott, P. Schurtenberger, and H. Siegmann, "Enormous yield of photoelectrons from small particles," *Phys. Rev. Lett.* **45**(15), pp. 1284–1287, 1980.
[32] R. K. Jain and R. C. Lind, "Degenerate four-wave mixing in Semiconductor-Doped Glasses," *J. Opt. Soc. Am.* **73**(5), pp. 647–653, 1983.
[33] S. S. Yao, C. Karaguleff, A. Gabel, R. Fortenberry, C. T. Seaton, and G. I. Stegeman, "Ultrafast Carrier and Grating Lifetimes in Semiconductor-Doped Glasses," *Appl. Phys. Lett.* **46**(9), pp. 801–802, 1985.
[34] F. Hache, D. Ricard, and C. Flytzanis, "Optical Nonlinearities of Small Metal Particles: Surface-Mediated Resonance and Quantum Size Effects," *J. Opt. Soc. Am. B* **3**(12), pp. 1647–55, 1986.
[35] S. Shafei, R. Lytel, and M. G. Kuzyk, "Geometry-controlled nonlinear optical response of quantum graphs," *ArXiv e-prints* , Aug. 2012.
[36] B. Tian, P. Xie, T. Kempa, D. Bell, and C. Lieber, "Single-crystalline kinked semiconductor nanowire superstructures," *Nat. Nanotech.* **4**(12), pp. 824–829, 2009.